INTERNATIONAL JOURNAL FOR NUMERICAL METHODS IN FLUIDS, VOL. 14, 793–815 (1992)

ENERGY FLUX EQUALIZATION: AN OPEN BOUNDARY CONDITION FOR NON-LINEAR FREE SURFACE FLOWS

SRIDHAR JAGANNATHAN

The Glosten Associates, Inc., 600 Mutual Life Building, 605 First Avenue, Seattle, WA 98104, U.S.A.

SUMMARY

In the simulation of non-linear free surface flows in a finite domain a major concern is with the radiation condition to be applied at the 'open' boundary. No general theoretical radiation conditions are known to exist. In this paper a new open boundary condition is formulated based on energy flux equalization between the non-linear inner domain and a linear outer domain. The non-linear flow in the inner domain is solved numerically using a semi-Lagrangian procedure. The energy flux arriving at the open boundary is removed using a new open boundary condition which acts as a linear wave absorber. For the cases studied the performance of this boundary condition is found to be quite good.

KEY WORDS Energy flux equalization Open boundary condition Non-linear free surface flows

1. INTRODUCTION

The use of linear hydrodynamic analysis has become quite commonplace and the results of such analysis are quite satisfactory for many engineering problems. Moreover, considering the essentially stochastic nature of the oceans, the use of linear analysis and hence superposition of solutions has led to the widespread use of spectral methods and impulse response function techniques. The domain equation for the velocity potential, assuming the fluid to be incompressible and the flow irrotational, is the Laplace equation, which is linear. Non-linearities are introduced into the problem through the boundary conditions at the free surface and on the body. In a linear solution these boundary conditions are linearized, leading to the requirements that the free surface elevation and the body remain in close proximity to their mean positions. This then precludes steep waves and large body motions. However, these non-linear effects are extremely important, particularly in the context of survivability at sea. There have been numerous cases of small vessels capsizing in rough seas. With the increasing number of offshore structures, appropriate methods of analysis are needed to evaluate the behaviour of such structures under extreme conditions to ensure safety at sea. In recent years considerable progress has been made in addressing free surface and body non-linearities directly in the time domain.[1,2]

The particular hydrodynamic problem of interest here is that of two-dimensional non-linear free surface flows in the horizontal–vertical plane. The method of solution is a semi-Lagrangian time-stepping procedure first used by Longuet-Higgins and Cokelet.[2] This procedure permits the satisfaction of the non-linear dynamic and kinematic free surface conditions. Vinje and Brevig[3] modified this procedure for solutions in the physical plane. This modified method is used as the basic method of solution in which the new boundary condition is embedded. The mathematical formulation for this solution technique is described in detail in Reference 4.

0271–2091/92/070793–23$11.50

Received 27 February 1989
Revised 24 June 1991

It is often necessary to introduce artificial boundaries to limit the domain of computation. Boundary conditions are then needed at these artificial boundaries to ensure a unique solution. Moreover, the 'open' boundary conditions should be such that the solution so obtained will closely approximate the solution that would exist in the absence of the artificial boundary, i.e. the open boundary conditions should not distort the solution in the interior domain. For non-linear free surface problems no general open boundary conditions are known so far. Many individual approaches have emerged, such as those of Hedstrom[5] for non-linear hyperbolic systems, Rudy and Strikwerda[6] for Navier–Stokes flows and Engquist and Majda[7] for a class of wave equations. A review of open boundary conditions is provided by Jagannathan.[8] In this paper a new open boundary condition based on energy flux equalization is proposed.

2. ENERGY CONSIDERATIONS

The problem of open boundaries may be posed in terms of the amount of energy that should be permitted to leave the computational domain through the open boundaries.[1] In a two-dimensional horizontal–vertical plane, consider a finite domain Ω and its boundary $\Sigma = \Sigma_L \cup \Sigma_B \cup \Sigma_A \cup \Sigma_F$, where Σ_L is a vertical plane on the left side, Σ_B is the bottom boundary, Σ_F is the free surface boundary and Σ_R is the open vertical boundary on the right side. Let free surface waves enter the domain through Σ_L and exit through Σ_R. Let E_Ω denote the total energy of fluid motion in the domain Ω. The energy theorem of John[9] (see also Reference 1) states

$$\dot{E}_\Omega = \rho \frac{\mathrm{d}}{\mathrm{d}t} \int_\Omega (\tfrac{1}{2}|\nabla\phi|^2 + gy)\mathrm{d}\Omega \tag{1}$$

$$= \int_\Sigma [p\upsilon_n - \rho\phi_t(\phi_n - \upsilon_n)]\mathrm{d}\Sigma, \tag{2}$$

where υ_n is the normal velocity of any physical boundary. Let $\dot{E}_L$ be the rate at which energy enters the domain through Σ_L. In view of the boundary conditions at Σ_L, Σ_B and Σ_F, equation (2) may be written as

$$\dot{E}_L = \dot{E}_\Omega + \int_{\Sigma_R} [p\upsilon_n - \rho\phi_t(\phi_n - \upsilon_n)]\mathrm{d}\Sigma, \tag{3}$$

since $\upsilon_n = \phi_n = 0$ for Σ_B; $p = 0$ and $\upsilon_n = \phi_n$ for Σ_F. The second term in equation (3) is the energy flux from the open boundary Σ_R. This boundary may be perceived either as a rigid movable boundary where $\phi_n = \upsilon_n$ or as an analytical open boundary without a physical boundary, i.e. $\upsilon_n = 0$. In any case, let E_R denote the energy flux at the open boundary Σ_R and hence we get

$$\dot{E}_L(t) - \dot{E}_\Omega(t) = \dot{E}_R(t), \tag{4}$$

i.e.

rate of energy input into the system − rate of energy capture by the system
= rate of energy flux from the system.

The integral of equation (4) is also equally valid:

$$E_L(t) - E_\Omega(t) = E_R(t), \tag{5}$$

i.e.

total energy input into the system − total energy captured by the system
= total energy flux from the system.

The choice of an open boundary condition would implicitly define the energy flux out of the open boundary and hence by equation (4) would also determine the energy accumulation inside the fluid domain. Thus an improper open boundary condition would lead to improper accumulation of energy in the domain (i.e. through reflections) and to a progressive deterioration of the solution. Equations (4) and (5) may be used to monitor the accuracy of the numerical solution. In particular, for steady state problems the average rate of energy input should equal the average rate of energy flux from the domain. It should, however, be noted that the occurrence of a steady state does not necessarily imply that the solution is correct. The application of improper boundary conditions during the approach to steady state could clearly lead to a false steady state solution for non-linear problems.

It is intuitively attractive to wonder whether an open boundary condition may be obtained using energy flux considerations. In Reference 8 this problem is approached from two viewpoints, namely that of energy flux maximization and that of energy flux equalization. In this paper we look at the energy equalization scheme, where the optimal motion of the absorption boundary is sought based on the consideration that the incident energy flux from the inner domain is equal to the energy flux radiated to the outer domain.

3. ENERGY FLUX SCHEMES FOR LINEAR PROBLEMS

Consider two-dimensional linear waves from $x=-\infty$ to be incident upon a termination at $x=0$. If the termination boundary were stationary then the waves would be reflected, causing standing waves. We seek the optimal motion of the termination boundary which, based on the principle of equalization of energy flux, would minimize reflection and give a progressive wave solution.

The velocity potential is required to satisfy

$$\nabla^2\phi=0 \qquad \text{in } \Omega, \tag{6}$$

$$\phi_y=0 \qquad \text{at } y=-h, \tag{7}$$

$$\phi_x=\dot{x}(y,t) \qquad \text{at } x=0. \tag{8}$$

Let us first consider that there is no termination boundary at $x=0$. The incident two-dimensional linear waves from $x=-\infty$ are allowed to pass unhindered to $x=\infty$. The normal velocity of the fluid particles at the plane $x=0$ is then given by $\phi_x(y,t)$. Consider now that at $x=0$ we impose a rigid termination boundary such that the normal velocity $\dot{x}(y,t)$ of this boundary equals the exact solution $\phi_x(y,t)$ of the incident wave in the absence of the termination boundary. Clearly the rest of the fluid would not 'know' that a rigid termination boundary has been imposed in the flow. All the incident energy is then 'absorbed' by the termination boundary and there is neither a reflection of progressive waves nor any local disturbance. This perfect absorber is possible if the exact behaviour of the wave is known. For general flows (linear or non-linear) the exact solution at the open boundary is not known and hence the exact termination boundary solution to be used is also not known. Suppose that, owing to this difficulty, we impose some arbitrary termination boundary, say a piston or hinge type in the simplest case. How then is the motion of this boundary to be obtained? The proposition advanced here is that the boundary motion is to be such as to equalize the incident flux to the radiated flux at the termination boundary. In this paper this proposition is examined for problems with simple termination boundaries. In general the termination boundary can have an infinite number of degrees of freedom. The analysis here will be restricted to one and two degrees of freedom.

3.1. Single degree of freedom

The termination boundary is considered to have a single degree of freedom and the analysis is carried out in the time domain.

The velocity potential is required to satisfy

(i) $$\nabla^2\phi=0 \quad \text{in } \Omega,$$

(ii) $$\phi_y=0 \quad \text{on } y=-h,$$

(iii) linearized free surface conditions,[10]

(iv) $$\phi_x(y,t)=a(t)\delta(y) \quad \text{at the termination boundary } x=0, \tag{9}$$

where $a(t)$ is the time-dependent part of the absorber velocity (to be determined) and $\delta(y)$ is the absorber shape function (which is chosen).

In particular we have: for a 'piston' wave absorber,

$$\delta(y)=1;$$

for 'hinged' wave absorber of height h hinged at $y=-h$,

$$\delta(y)=(y+h)/h.$$

Let the total velocity potential be

$$\phi(x,y,t)=\phi_I+\phi_D+\phi_R, \tag{10}$$

where ϕ_I is the imposed incident velocity potential such as due to a small-amplitude Airy wave,[10] ϕ_D is the diffracted velocity potential due to the presence of the termination boundary and ϕ_R is the radiated velocity potential due to the motion of the termination boundary, satisfying conditions (i)–(iii) above and the condition at $x=0$ as

$$\phi_{Rx}=\dot{a}(t)\delta(y), \qquad \phi_{Dx}=-\phi_{Ix}.$$

Following Cummins,[11] the solution for ϕ_R is

$$\phi_R(x,y,t)=\dot{a}(t)\phi^*(x,y)+\int_{-\infty}^{t}\gamma(t-\tau)\dot{a}(\tau)\mathrm{d}\tau, \tag{11}$$

where ϕ^* denotes the instantaneous contribution and $\gamma(\tau)$ the delayed contribution to the velocity potential arising from the motion of the wave absorber.

The pressure due to ϕ_R is

$$p=-\rho\frac{\partial\phi_R}{\partial t}. \tag{12}$$

The hydrodynamic 'force' on the wave absorber is therefore

$$-F_O=\int_{-h}^{0}p\delta(y)\mathrm{d}y \tag{13}$$

$$=\ddot{a}(t)\rho\int_{-h}^{0}\phi^*\delta(y)\mathrm{d}y+\rho\int_{-h}^{0}\delta(y)\,\mathrm{d}y\int_{-\infty}^{t}\frac{\partial\gamma(t-\tau)}{\partial t}\dot{a}(\tau)\mathrm{d}\tau. \tag{14}$$

This can be written as

$$-F_O=M_h\ddot{a}(t)+\int_{-\infty}^{t}K(t-\tau)\dot{a}(\tau)\mathrm{d}\tau, \tag{15}$$

where

$$M_h=\rho\int_{-h}^{0}\phi^*\delta(y)\mathrm{d}y=\text{'genuine' added mass,}$$

$$K(t-\tau)=\rho\int_{-h}^{0}\frac{\partial\gamma(t-\tau)}{\partial t}\delta(y)\mathrm{d}y=\text{retardation function.}$$

Rather than solve for M_h and $K(\tau)$ directly as shown above, it is more convenient to solve for them on the basis of the frequency domain added mass and damping coefficients for the wave absorber as detailed in Appendix I.

Let the wave excitation force on the absorber from the inner domain be

$$F_I(t)=-\rho\int_{-h}^{0}(\phi_{It}+\phi_{Dt})\delta(y)\mathrm{d}y. \tag{16}$$

Clearly the work done on the absorber from the inner domain due to the incident potential is $F_I(t)\dot{a}(t)$. The work done by the absorber into the outer domain is due only to the radiation potential, which equals $-F_O(t)\dot{a}(t)$. Equalizing the incident work to the radiated energy, we get from equations (15) and (16)

$$M_h\ddot{a}(t)+\int_{-h}^{t}K(t-\tau)\dot{a}(\tau)\mathrm{d}\tau=F_I(t). \tag{17}$$

This is an integro-differential equation for the optimal motion $a(t)$ which equalizes the incident energy flux to the radiated energy flux.

3.2. Two degrees of freedom

The termination boundary is considered to have two degrees of freedom and the analysis is carried out in the time domain.

The velocity potential is required to satisfy

(i) $$\nabla^2\phi=0 \quad \text{in } \Omega, \tag{18}$$

(ii) $$\phi_y=0 \quad \text{on } y=-h, \tag{19}$$

(iii) linearized free surface conditions,

(iv) $$\phi_x(y,t)=\dot{a}_1(t)\delta_1(y)+\dot{a}_2(t)\delta_2(y), \tag{20}$$

where $a_i(t)$ is the time-dependent part of the absorber velocity in d.o.f. i and $\delta_i(y)$ is the absorber shape function for d.o.f. i.

Let the total velocity potential be

$$\phi(x,y,t)=\phi_I+\phi_D+\phi_R^{(1)}+\phi_R^{(2)}, \tag{21}$$

where $\phi_R^{(i)}$ is the radiated velocity potential of the absorber in d.o.f. i, satisfying conditions (i)–(iii) above and the condition at $x=0$ as

$$\phi_{Rx}^{(1)}=\dot{a}_1(t)\delta_1(y), \qquad \phi_{Rx}^{(2)}=\dot{a}_2(t)\delta_2(y), \qquad \phi_{Dx}=-\phi_{Ix}.$$

As before, the radiation potentials may be represented as

$$\phi_R^{(1)}=\dot{a}_1(t)\phi_1^*(x,y)+\int_{-\infty}^{t}\gamma_1(t-\tau)\dot{a}_1(\tau)\mathrm{d}\tau, \tag{22}$$

$$\phi_R^{(2)} = \dot{a}_2(t)\phi_2^*(x, y) + \int_{-\infty}^{t} \gamma_2(t-\tau)\dot{a}_2(\tau)\mathrm{d}\tau, \tag{23}$$

Let us define

$$-F_{ij} = \int_{-h}^{0} p_j \delta_i(y)\mathrm{d}y = -\rho \int_{-h}^{0} \frac{\partial \phi_R^{(j)}}{\partial t} \delta_i(y)\mathrm{d}y = M_{ij}\ddot{a}_j + \int_{-\infty}^{0} K_{ij}(t-\tau)\dot{a}_j(\tau)\mathrm{d}\tau \tag{24}$$

(summation convention not implied), where

$$M_{ij} = \rho \int_{-h}^{0} \phi_j^* \delta_i(y)\mathrm{d}y = \text{'genuine' added mass},$$

$$K_{ij}(t-\tau) = \rho \int_{-h}^{0} \frac{\partial \gamma_j(t-\tau)}{\partial t} \delta_i(y)\mathrm{d}y = \text{retardation function}. \tag{25}$$

Let

$$F_{il}(t) = -\rho \int_{-h}^{0} (\phi_{It} + \phi_{Dt})\delta_i(y)\mathrm{d}y \tag{26}$$

be the excitation force on the absorber in mode i from the inner domain.

M_{ij} and K_{ij} may be obtained from the frequency domain added mass and damping coefficients as shown in Appendix I. The energy flux equalization process for the *degree of freedom* i then yields

$$M_{ij}\ddot{a}_j(t) + \int_{-\infty}^{0} K_{ij}(t-\tau)\,\dot{a}_j(\tau)\,\mathrm{d}\tau = F_{il}(t) \tag{27}$$

(tensor notation for index repetition used). This is a pair of coupled linear integro-differential equations for the optimal motions in two degrees of freedom which equalizes the incident and radiated energy fluxes.

4. ENERGY FLUX EQUALIZATION FOR NON-LINEAR PROBLEMS

In the previous section the optimal motion of the linear absorber with a linear forcing function from the inner domain is given by equation (27). We propose to extend this formulation for non-linear waves generated in the inner domain shown in Figure 1.

Consider now the energy flux incident upon the termination boundary from the inner domain. If at any instant in time $\phi(t)$ represents the velocity potential at the termination boundary, then we have for a single-degree-of-freedom wave absorber

$$\phi_x(y, t) = \dot{a}(t)\delta(y).$$

The energy flux from the inner domain is given by

$$\dot{E}_I(t) = \int_{-h}^{\eta(t)} p\phi_x \mathrm{d}y = \int_{-h}^{\eta(t)} p\dot{a}(t)\delta(y)\,\mathrm{d}y = \dot{a}(t)\int_{-h}^{\eta(t)} p\delta(y)\,\mathrm{d}y = \dot{a}(t)F_I(t), \tag{28}$$

where

$$F_I(t) = \int_{-h}^{\eta(t)} p\delta(y)\,\mathrm{d}y$$

is the hydrodynamic 'force' on the wave absorber from the inner domain.

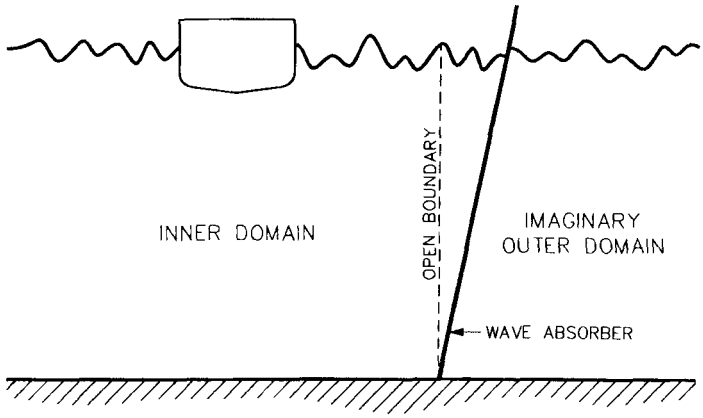

Figure 1. Definition sketch

Equating the energy flux from the inner domain to the energy flux into the outer domain, we get

$$\dot{E}_O(t) = \dot{E}_I(t),$$

and hence from equations (15) and (28):

$$-\dot{a}(t)F_O(t) = \dot{a}(t)F_I(t),$$

i.e.

$$M_h\ddot{a}(t) + \int_{-\infty}^{t} K(t-\tau)\dot{a}(\tau)\,d\tau = F_I(t). \tag{29}$$

This is an integro-differential equation for the optimal motion $a(t)$ of the wave absorber which equalizes the incident energy flux to the radiated energy flux at every instant in time.

Similarly, for the two degree-of-freedom wave absorber we have

$$\dot{E}_O(t) = \sum_{i=1}^{2} F_{iI}(t)\dot{a}_i(t), \tag{30}$$

where

$$F_{iI}(t) = \int_{-h}^{\eta(t)} p\delta_i(y)\,dy.$$

Hence, analogously to equation (27) we get

$$M_{ij}\ddot{a}_j(t) + \int_{-\infty}^{t} K_{ij}(t-\tau)\dot{a}_j(\tau)\,d\tau = F_{iI}(t). \tag{31}$$

Note that in equation (29) the left-hand side denotes the hydrodynamic force due to a linear outer domain problem and the right-hand side denotes the forcing function from a non-linear inner domain problem. The extension to a non-linear outer domain is possible using a Volterra kernel approach for the wave absorber.

For the non-linear case we may say in general that

$$-F_0 = Y(\ddot{a}(t), \dot{a}(t)) \quad \text{for } t>0, \tag{32}$$

where Y is a functional of the functions $\ddot{a}(t)$ and $\dot{a}(t)$. In correspondence with equation (27) for the linear case, our hypothesis is that the optimal motion of the wave absorber for the non-linear case may be obtained as the solution of

$$Y(\ddot{a}(t), \dot{a}(t)) = F_1(t). \tag{33}$$

The determination of the functional Y has received some attention in hydrodynamics. For a ship of mass m the solution for motion in yaw was assumed by Bishop *et al.*[12,13] in the form

$$m\ddot{y}_1 = Y(y_1(t)). \tag{34}$$

This functional Y was then assumed expandable in a Volterra series as

$$Y = \int_0^\infty Y_v(\tau)\dot{y}_1(t-\tau)\mathrm{d}\tau + \int_0^\infty Y_{\dot{v}}(\tau)\ddot{y}_1(t-\tau) + \int_0^\infty \int_0^\infty Y_v(\tau_1\tau_2)\dot{y}_1(t-\tau_1)\dot{y}_1(t-\tau_2)\mathrm{d}\tau_1\mathrm{d}\tau_2 + \ldots . \tag{35}$$

However, the hydrodynamic problems associated with the determination of the Volterra kernels were not formulated by the authors.

The solution for $Y(t)$ may be obtained by applying the analysis of Guo,[14] whose solution consisted of a set of integral equations in terms of the time-dependent Green function. It may also be possible to obtain the solution using higher-order transforms as follows.

In general the Volterra series operator with kernels h_n may be given as

$$Ya(t) = \sum_{n=1}^{\infty} y_n(t), \tag{36}$$

where

$$y_n(t) = \int_{n\text{-fold}} \ldots \int h_n(\tau_1, \ldots, \tau_n) a(t-\tau_1) \ldots a(t-\tau_n)\mathrm{d}\tau_1 \ldots \mathrm{d}\tau_n. \tag{37}$$

The Laplace transform of the kernels is defined as

$$H_n(s_1, \ldots, s_n) = \int \ldots \int h_n(\tau_1, \ldots, \tau_n)\exp[-(s_1\tau_1 + \ldots + s_n\tau_n)]\,\mathrm{d}\tau_1 \ldots \mathrm{d}\tau_n, \tag{38}$$

where H_n is denoted the nth frequency domain kernel.

Suppose the input is a multitone given by

$$a(t) = \sum_{i=1}^{K} \alpha_i \exp(s_i t); \tag{39}$$

then the solution for the nth-order component is

$$y_{sn}(t) = \sum_{i_1=1}^{K} \sum_{i_2=1}^{K} \ldots \sum_{i_n=1}^{K} \alpha_{i_1}\alpha_{i_2} \ldots \alpha_{i_n} \exp\left[\sum_{j=1}^{n} s_{i_j} t\right] H_n(s_{i_1}, s_{i_2}, \ldots, s_{i_n}). \tag{40}$$

The Fourier transform components are obtained from the above with $s = \pm j\omega$. In particular, if $K=1$ (i.e. the input is only at frequency ω and amplitude α), then the solution to first order is at frequency ω, the solution to second order contains frequencies 0, 2ω and so on.

For our wavemaker problem we suggest that the Volterra kernel h_n may be obtained as

$$h_n(\tau_1, \ldots, \tau_n) = \int \ldots \int H_n(s_1, \ldots, s_n) \exp[-(s_1\tau_1 + \ldots + s_n\tau_n)] \, ds_1 \ldots ds_n, \tag{41}$$

where the $H_n(s_1, \ldots, s_n)$ are obtained from the frequency domain boundary value problems up to the desired order. It may be noted that this is the procedure followed for the first order and the generalization here is for higher orders.

5. NUMERICAL SOLUTION PROCEDURE

The solution to the non-linear forced body motion problem in the inner computational domain is based on simulation with discretization in both space and time. As defined in Section 2, the right-side boundary Σ_R is taken as an open boundary. In the present case the open boundary is taken to be a single-degree-of-freedom *linear* wave absorber whose motion is determined on the basis of equation (33). For this two-dimensional problem, with potential theory being applicable (the fluid being considered inviscid and incompressible and the flow irrotational), the fluid motions are described using the complex velocity potential β. The contour C of the domain is divided into elements with the variable of interest (β or β_t) being defined at nodal points. The part of the contour where the velocity potential ϕ is known is denoted C_ϕ and where the streamfunction ψ is known it is denoted C_ψ (and similarly for ϕ_t and ψ_t). When the body is in the interior of the domain, a 'branch cut' is taken out to the body to permit the latter to be considered part of the boundary for computational purposes. Details of the numerical solution procedure are given by Jagannathan.[4]

The process of simulation can be described in terms of two stages for each time step: (a) solution of a well-posed boundary value problem for β (and β_t) at a fixed instant in time and (b) evolution of variables all over C to set up the boundary value problem for the next instant in time.

The retardation function is determined as shown in Appendices I and II, with a high-frequency approximation for the damping coefficient beyond a frequency σ_H:

$$K(\tau) = \frac{2}{\pi} \int_0^{\sigma_H} b(\sigma) \cos(\sigma\tau) d\sigma + \frac{2}{\pi} \int_{\sigma_H}^{\infty} b_H(\sigma) \cos(\sigma\tau) d\sigma \tag{42}$$

and

$$b_H(\sigma) \approx \frac{2\rho g^2}{\sigma^3} \quad \text{for } \sigma > \sigma_H, \tag{43}$$

where $b(\sigma)$ is the damping coefficient for the wave absorber.

The following steps may be used to implement the open boundary condition.

(*a*) *Choose wave absorber*

Choose the kind of wave absorber in terms of its shape function and number of degrees of freedom—e.g. a hinged plate attached to the bottom.

(*b*) *Obtain frequency domain characteristics*

Obtain the wave absorber's frequency domain characteristics in terms of its wavemaking into the outer domain. These are the added mass and damping coefficients $m_h(\sigma)$ and $b(\sigma)$.

For the hinged plate these are explicitly derived as equations (55) and (56) and are shown in Figures 2 and 3.

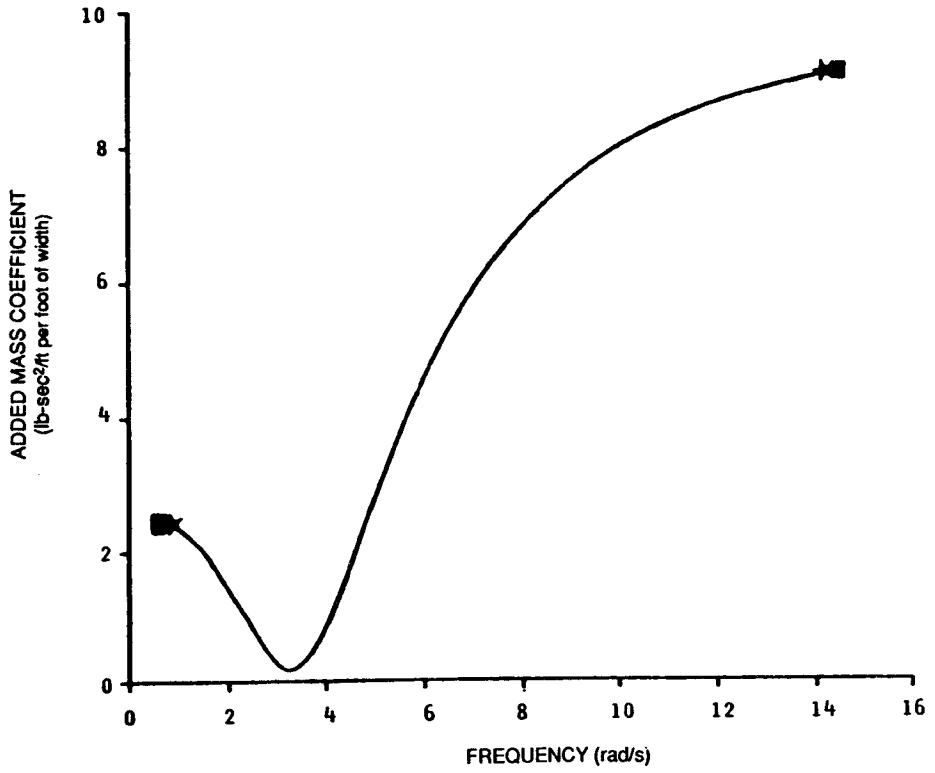

Figure 2. Added mass coefficient for wave absorber (hinged type): ■, frequency domain solution; ★, impulse response solution

(*c*) *Obtain time domain characteristics*

The time domain characteristics of a system can be obtained from its frequency domain characteristics by convolution. The time domain retardation function defines the system response due to impulsive motion and is obtained from the frequency domain added mass and damping behaviour. Equations (45) show the derivation of the retardation function based on $b(\sigma)$ and $m(\sigma)$.

For the hinged absorber, since $b(\sigma)$ and $m(\sigma)$ are explicitly known, we can obtain the retardation function $K(\tau)$ and the 'genuine' added mass M_h. The latter is a single value whereas the retardation function depends on the time lag τ. As can be seen from equation (17), the retardation function $K(\tau - a)$ denotes the hydrodynamic force on the wavemaker at time τ due to a unit velocity at time τ.

Once we know M_h and $K(\tau)$, we are ready to solve any kind of inner domain problem with our wave absorber as the open boundary.

(*d*) *Solve inner domain problem at time* τ

Solve the inner domain problem detailed in Reference 4 at some time t with the open boundary condition being the *known* velocity of the wave absorber at time τ. Hence obtain the forcing function $F_1(t)$ such as given by equation (28). In effect, the interior solution is forcing the wave absorber to respond.

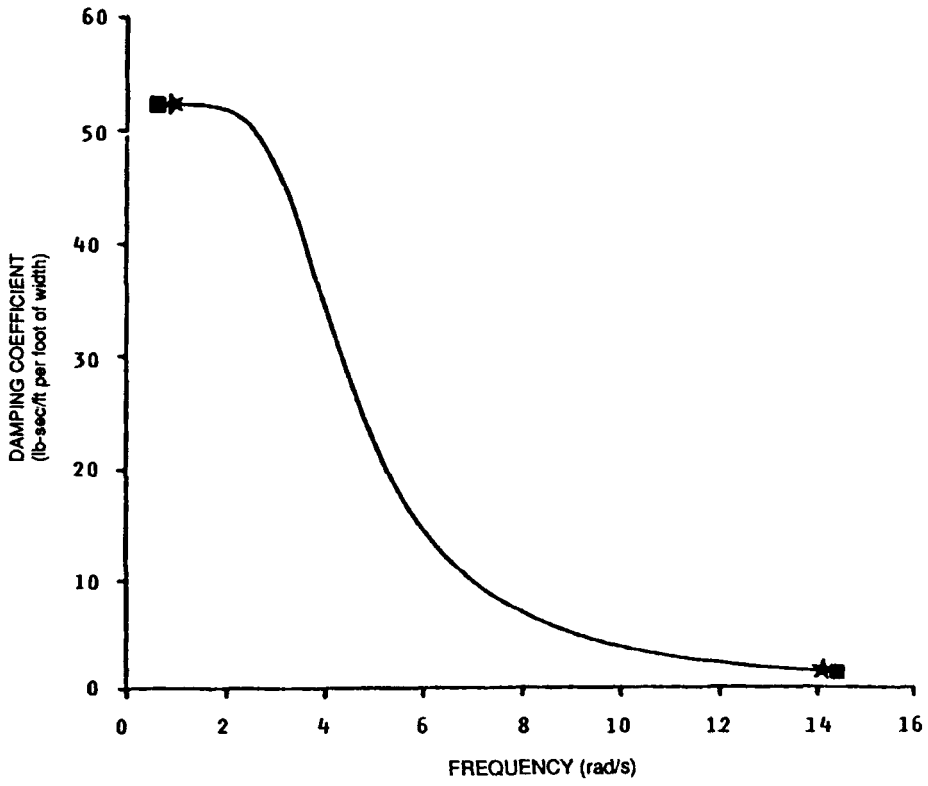

Figure 3. Damping coefficient for wave absorber (hinged type): ■, frequency domain solution; ★, impulse response solution

(*e*) *Solve for wave absorber motion at time* $\tau + \Delta\tau$

Solve the wave absorber velocity at time $\tau + \Delta\tau$ using equation (29). Note that M_h, $K(t-\tau)$, $\dot{a}(\tau)$ and $F_I(t)$ are known. Hence the acceleration $\ddot{a}(\tau)$ can be obtained that yields the velocity $\dot{a}(\tau + \Delta\tau)$ for use at time $\tau + \Delta\tau$.

(*f*) *Repeat steps* (*d*) *and* (*e*)

Repeat steps (d) and (e) to obtain the solution to the problem. Suitable checks, such as energy balances and wave reflections, may be used to monitor the fluid behaviour in the inner domain.

6. RESULTS AND DISCUSSION

To investigate the efficiency of the energy flux equalization procedure, a forced wavemaker problem was chosen. The left-side boundary is considered in hinged-type wavemaker with a forced sinusoidal motion of amplitude 0·005 ft at a frequency of 3 rad s^{-1} in water of depth 7 ft. The energy flux equalization procedure to be applied at the right-side wave absorber is based on Section 3 and corresponds to the velocity potential in the outer domain satisfying linearized free surface conditions. However, the forcing function derived at the open boundary (i.e. at the wave absorber) is based on the non-linear inner domain where non-linear free surface and body

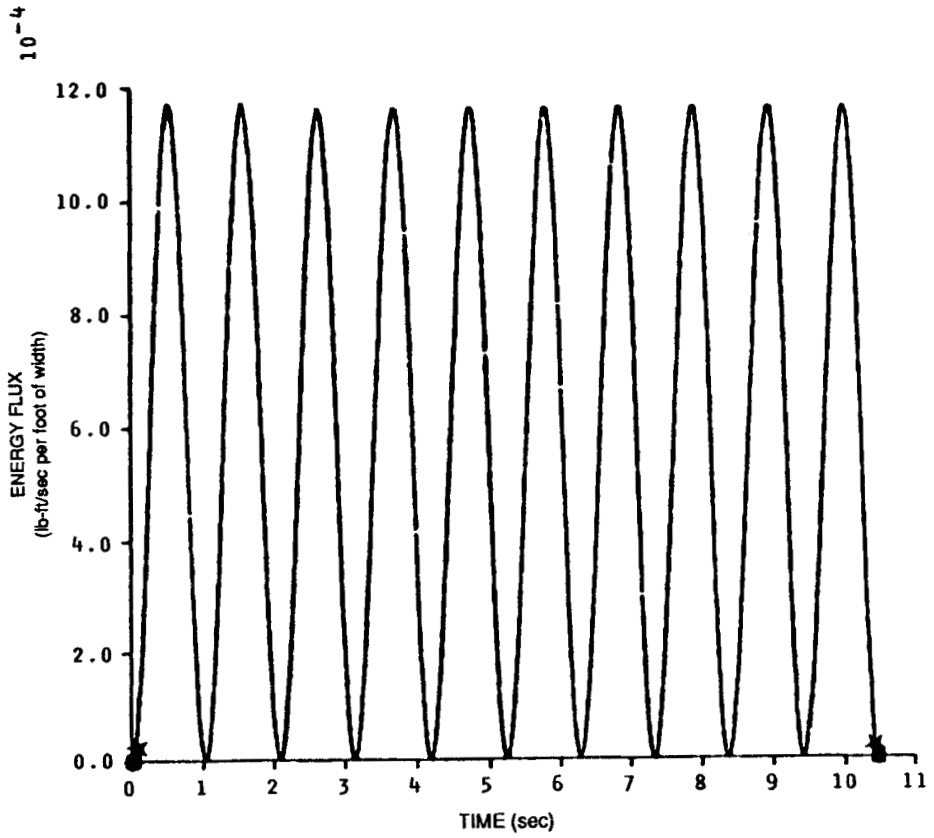

Figure 4. Energy absorption for optimal motion (hinged type): ■, optimal energy absorbed; ★, incident energy

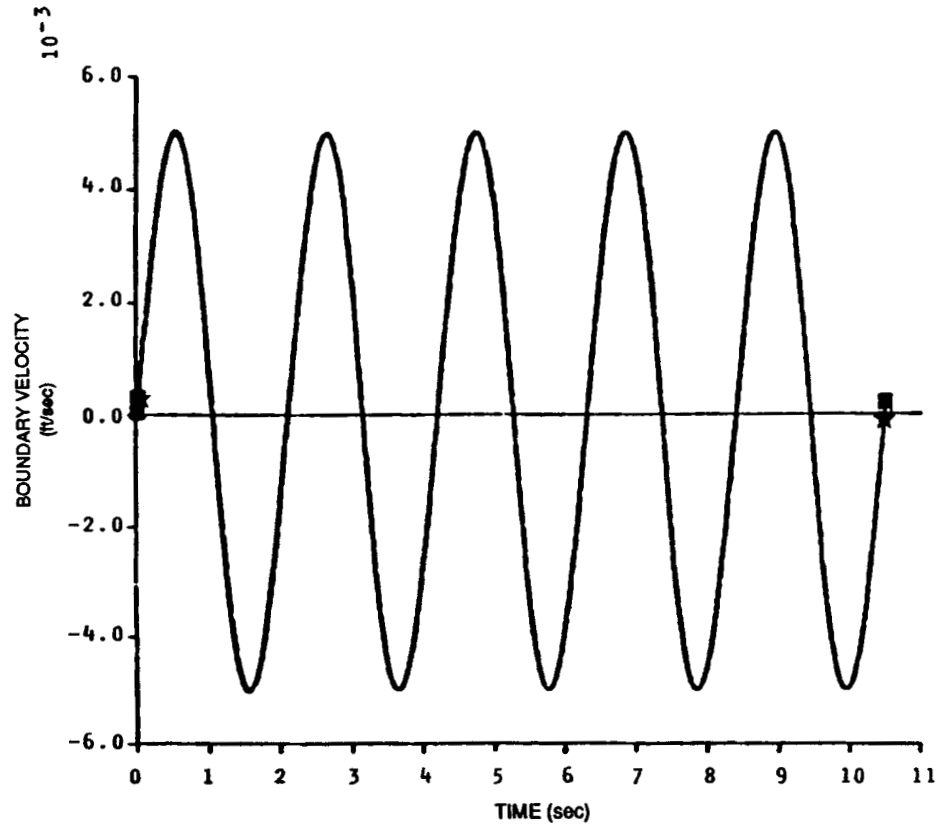

Figure 5. Optimal motion of wave absorber (hinged type): ■, impulse response solution; ★, frequency domain solution

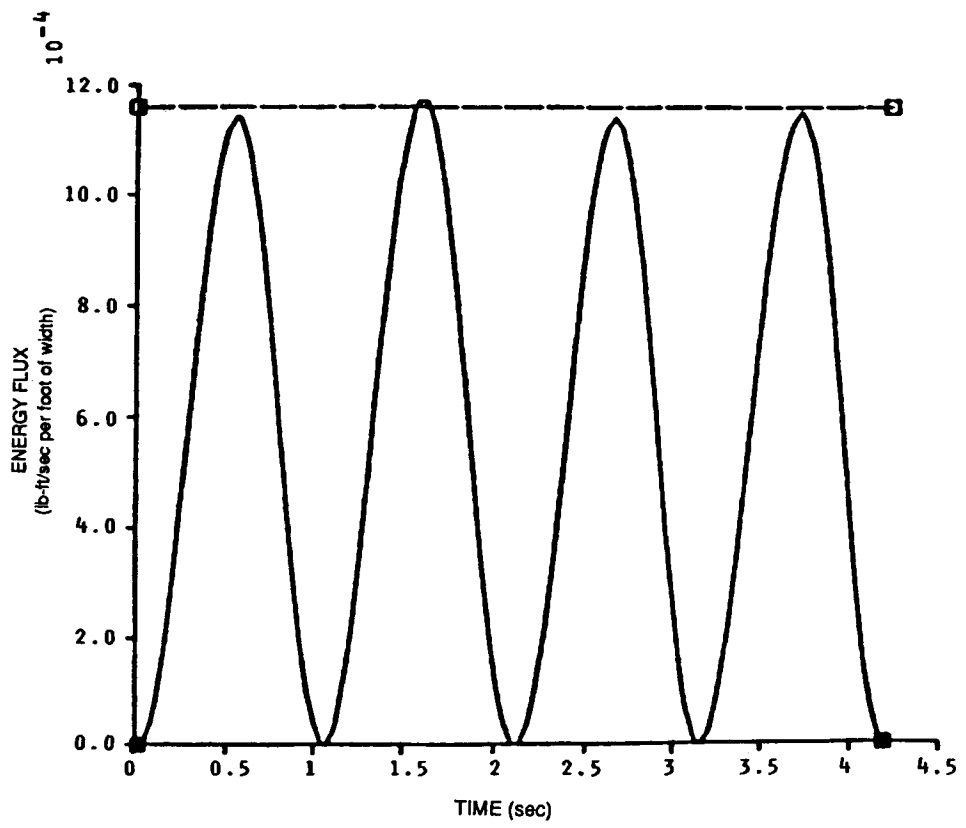

Figure 6. Energy input by port-side wave maker (hinged type): ■, non-linear simulation; □, frequency domain amplitude

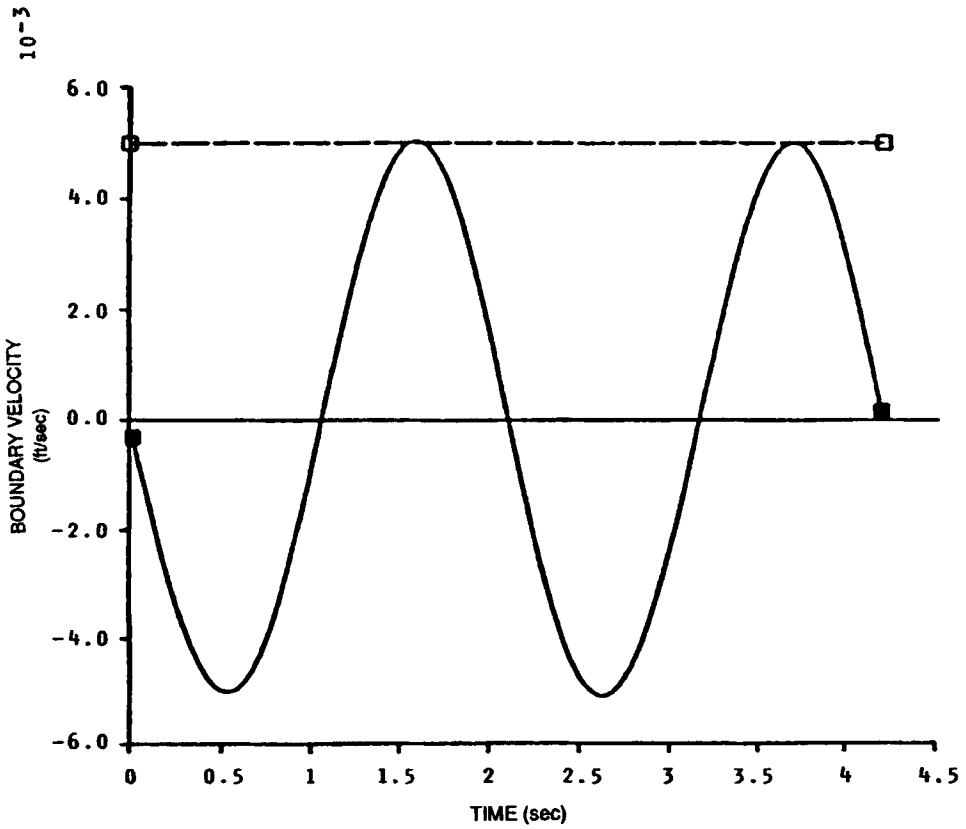

Figure 7. Optimal absorber boundary motion (hinged type): ■, non-linear simulation; □, frequency domain amplitude

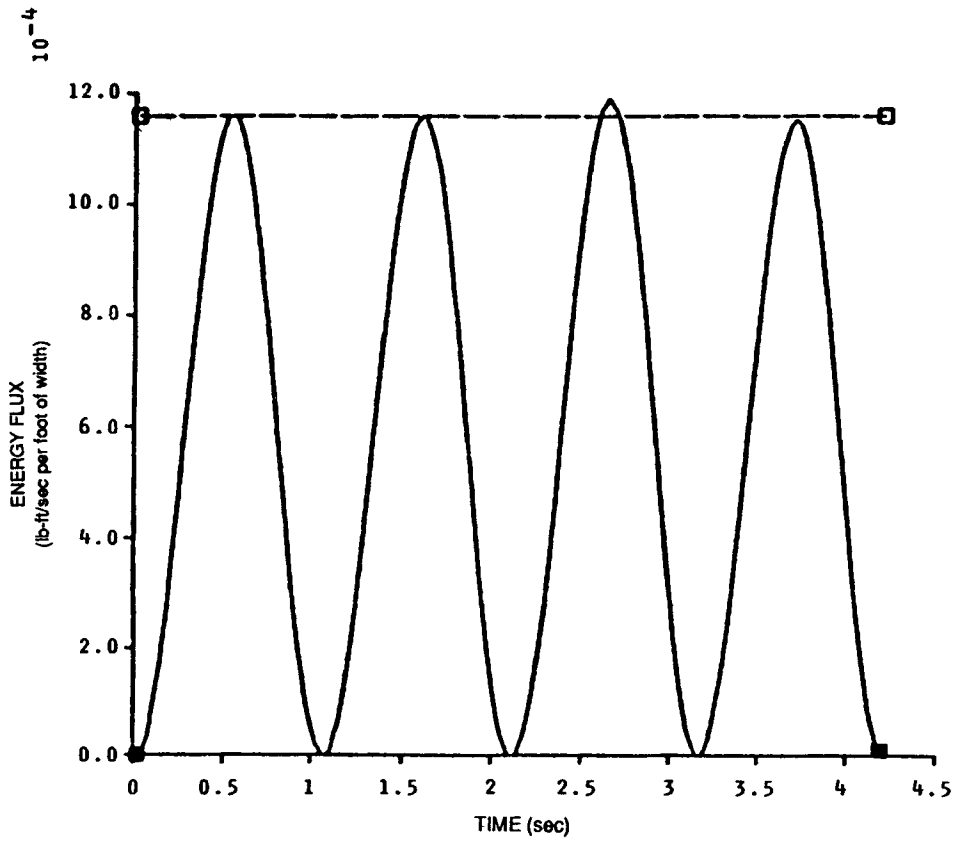

Figure 8. Energy absorbed for optimal boundary motion (hinged type): ■, non-linear simulation; □, frequency domain amplitude

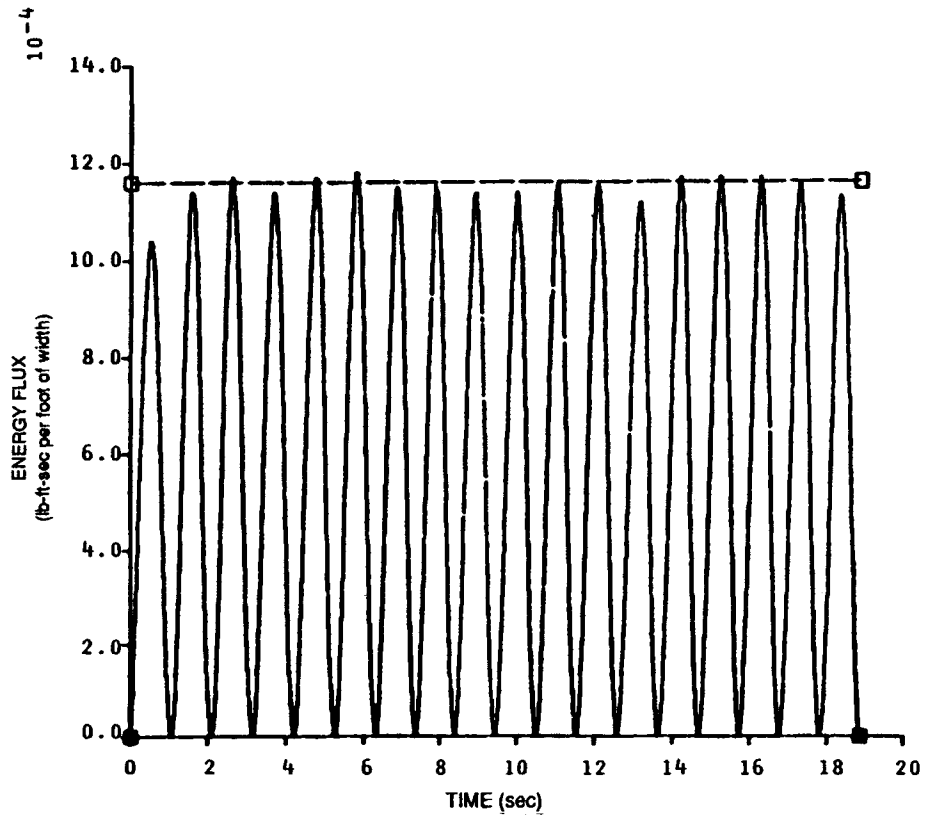

Figure 9. Energy input by port-side wavemaker (hinged type): ■, non-linear simulation; □, frequency domain amplitude

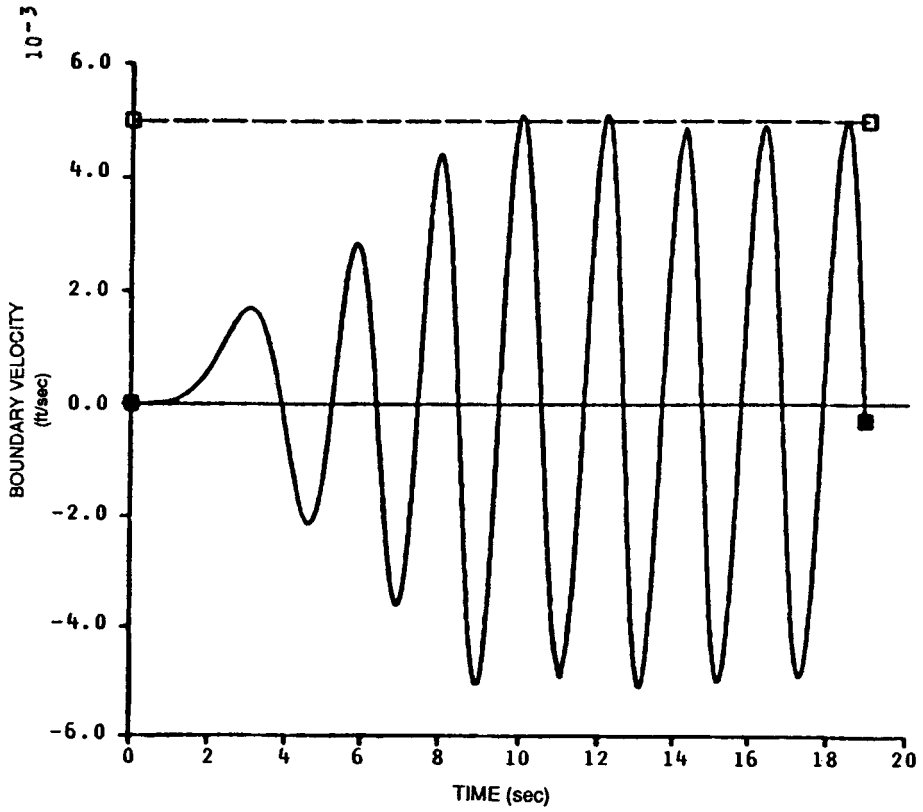

Figure 10. Optimal absorber boundary motion (hinged type): ■, non-linear simulation; □, frequency domain amplitude

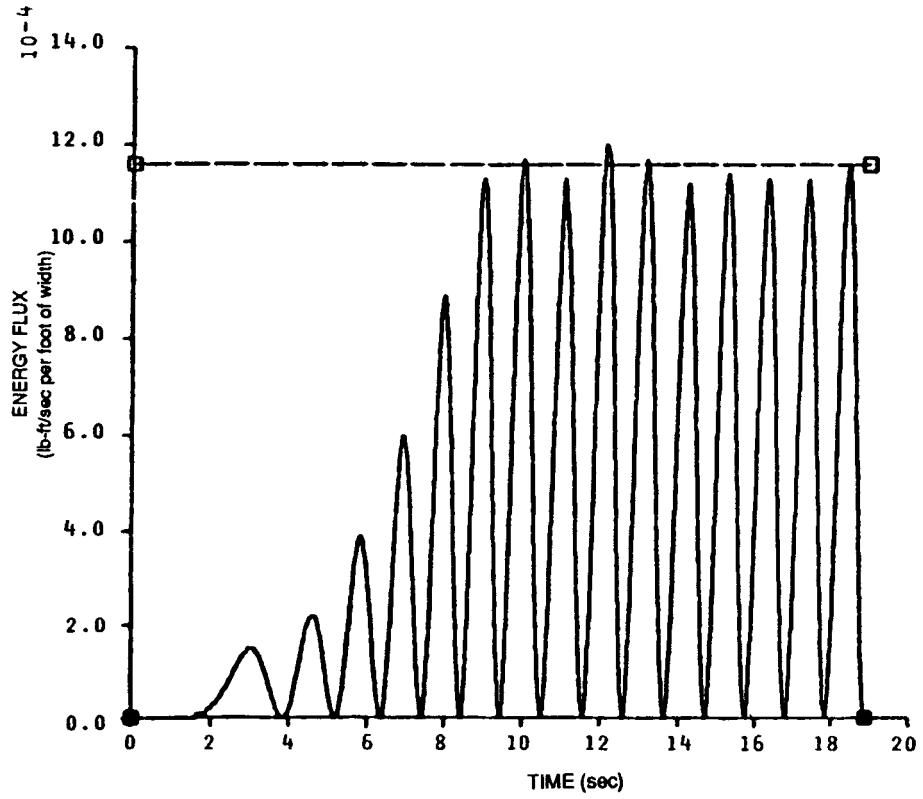

Figure 11. Energy absorbed for optimal boundary motion (hinged type): ■, non-linear simulation; □, frequency domain amplitude

conditions are satisfied. Figures 2 and 3 show the added mass and damping function for the linear absorber, derived using two methods: the frequency domain solution (■) and the impulse response solution (★). The two solutions are practically identical, indicating that the retardation function is accurate. Figures 4 and 5 shows the energy absorption and optimal boundary motion for a sinusoidal forcing function corresponding to a standing wave given by equation (19). The frequency domain and impulse response solutions are seen to be identical. The energy flux amplitude ratio L is 0·017 for this case[8] and the absorption characteristics are clearly quite good. Our aim now is to incorporate this absorber into the non-linear simulation procedure.

The length of the inner domain is chosen as 1·5 times the wavelength corresponding to the frequency of oscillation of the left-side wavemaker. A free surface wave corresponding to the amplitude of the wavemaker motion is imposed at $t=0$. The expected solution of the starboard-side absorber is a motion antisymmetric with respect to the wavemaker. One hundred equally spaced nodes were used on the free surface, 28 nodes on each side boundary and 20 nodes at the bottom. Figure 6 shows the energy input to the domain by the wavemaker. Figure 7 shows the response of the wave absorber derived with the forcing function obtained from the non-linear simulation procedure. The corresponding energy absorbed by the open boundary is given in Figure 8. Clearly the optimal boundary motion and energy absorption compare quite well with the frequency domain solutions.

The same problem was then repeated with no initial free surface elevation. The wavemaker starts from rest. Figure 9 shows the energy input by the wavemaker to the domain. The optimal motion of the absorber is given in Figure 10. The amplitude of motion approximately equals the frequency domain solution, but some slight peaks and troughs are noticeable. The energy absorbed corresponding to this motion is shown in Figure 11. The comparison here with the frequency domain solution is fair, with the occurrence of peaks and troughs more evident. This is because the energy flux varies as the square of the motion and the errors are thereby made more evident. The error in the boundary motion is less than 2% and that in the energy flux about 4%.

The numerical procedure was found to be sensitive to the method of integration as well as to the resolutions in space and time. The evolution of the free surface in time was solved simultaneously with the optimal motion of the absorber with a fourth-order Runge–Kutta algorithm. The time step used was one-hundredth of the oscillation period. The intersection of the absorber with the free surface gives rise to a logarithmic singularity which has to be treated properly, since the free surface elevation at that intersection point contributes to the forcing function for the absorber motion. At the intersection point the velocity potential is obtained from the free surface condition and the streamfunction from the absorber (i.e. the intersection point is fully determinate in terms of the boundary value problem). It is found that the vertical velocity of the intersection node is best approximated by backward spatial differentiation of the velocity potential along the absorber rather than backward differentiation along the free surface or complex differentiation around the intersection.

7. CONCLUDING REMARKS

A general open boundary condition for non-linear free surface flows has been formulated based on the consideration of energy flux equalization between an inner non-linear computational domain and an external linear flow field. The procedure for linear single- and two-degree-of-freedom wave absorbers has been detailed, with the optimal solution obtained in the form of coupled integro-differential equations. The extension to non-linear wave absorbers has been formulated.

The performance of the open boundary condition based on energy flux equalization is quite good for the non-linear free surface problems that were investigated. For the case of the unsteady wavemaker problem the approach to the steady state is monotonic and the steady state is maintained with some low-frequency oscillation. Further numerical experiments will be required to study the systematic improvements in this procedure associated with choice of shape functions and the number of degrees of freedom of the wave absorber.

ACKNOWLEDGEMENTS

This work forms a part of the author's Ph.D. Dissertation[8] and was done under the guidance of Professor W. C. Webster, which is gratefully acknowledged. The author would like to thank Professor Ronald Yeung for his advice and assistance. The financial support given by the Department of Naval Architecture and Offshore Engineering, University of California, Berkeley is acknowledged with gratitude.

APPENDIX I: TIME DOMAIN ADDED MASS AND RETARDATION FUNCTION

Let indices i and j denote two degrees of freedom for the absorber. The 'genuine' added mass M_{ij} and retardation function K_{ij} in mode i for operation in mode j are defined as

$$M_{ij} = -\rho \int_{-h}^{0} \phi_j^* \delta_i(y) \mathrm{d}y, \qquad K_{ij}(t-\tau) = -\rho \int_{-h}^{0} \frac{\partial \gamma_j(t-\tau)}{\partial t} \delta_i(y) \mathrm{d}y, \tag{44}$$

where h is the water depth, $\delta_i(y)$ is the shape function in mode i and ϕ_j^* and γ_j are parts of the radiation potential as defined in equations (22) and (23).

Following Cummins,[11] the correspondence with frequency domain coefficients is invoked to obtain

$$K_{ij}(\tau) = \frac{2}{\pi} \int_0^{\infty} b_{ij}(\sigma) \cos(\sigma\tau) \mathrm{d}\sigma, \qquad M_{ij} = m_{ij}(\sigma_1) + \frac{1}{\sigma_1} \int_0^{\infty} K_{ij}(t-\tau) \sin(\sigma_1 \tau) \mathrm{d}\tau, \tag{45a,b}$$

where m_{ij} is the frequency domain added mass for the absorber in modes i and j, b_{ij} is the frequency domain damping coefficient for the absorber in modes i and j and σ_1 is any arbitrary frequency.

The frequency domain added mass and damping coefficients are obtained as follows. Let the absorber with shape function $\delta_j(y)$ execute simple harmonic motion at frequency σ (Figure 12):

$$\dot{x}(y, t) = \delta_j(y) \cos(\sigma t).$$

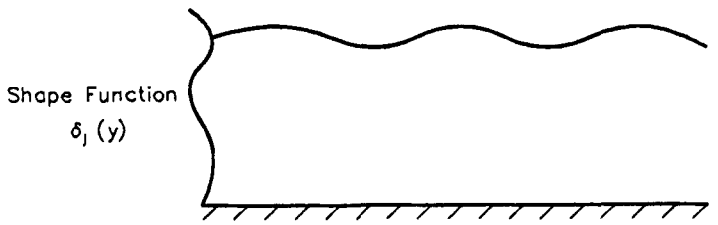

Figure 12. Definition sketch for wave absorber BVP

The solution for the velocity potential satisfying the domain equation and boundary conditions at the free surface, at the bottom and at infinity is[10]

$$\phi^{(j)} = b_{0j}\psi_0 \cos(k_0 x - \sigma t) + \sum_{n=1}^{\infty} b_{nj}\psi_n e^{-k_n x} \sin(\sigma t), \tag{46}$$

where

$$\sigma^2 = gk_0 \tanh(k_0 h), \qquad \sigma^2 = gk_n \tan(k_n h),$$
$$\psi_0(y) = \cosh[k_0(y+h)], \qquad \psi_n(y) = \cos[k_n(y+h)], \qquad n = 1, \ldots, \infty.$$

The boundary condition at $x = 0$ is

$$\phi_x^{(j)} = \dot{x}(y, t) = -\sigma\delta_j(y)\sin(\sigma t). \tag{47}$$

Hence, using equations (46) and (47) and the consideration of orthogonality of the functions $\psi_0(y)$ and $\psi_n(y)$, we get

$$b_{0j} = -\frac{\sigma}{k_0}\frac{I_{0j}^{(2)}}{I_0^{(1)}}, \qquad b_{nj} = \frac{\sigma}{k_n}\frac{I_{nj}^{(2)}}{I_n^{(1)}}, \tag{48a}$$

where

$$I_{0j}^{(2)} = \int_{-h}^{0} \delta_j(y)\psi_0(y)\mathrm{d}y, \qquad I_{nj}^{(2)} = \int_{-h}^{0} \delta_j(y)\psi_n(y)\mathrm{d}y,$$
$$I_0^{(1)} = \int_{-h}^{0} \psi_0^2(y)\mathrm{d}y, \qquad I_n^{(1)} = \int_{-h}^{0} \psi_n^2(y)\mathrm{d}y, \qquad n = 1, \ldots, \infty. \tag{48b}$$

The pressure at $x = 0$ is

$$p_i = -\rho\phi_t^{(j)} = \rho\sigma b_{0j}\psi_0 \sin(\sigma t) - \rho \sum_{n=1}^{\infty} \sigma b_{nj}\psi_n \cos(\sigma t). \tag{49}$$

The hydrodynamic force F_{ij} in mode i due to pressure in mode j is defined as

$$F_{ij} = \int_{-h}^{0} p_j \delta_i(y)\mathrm{d}y, \tag{50}$$

where $\delta_i(y)$ is the shape function of the absorber in mode i. Using equation (49) in equation (50), we have

$$F_{ij} = m_{ij}(\sigma)[-\sigma^2 \cos(\sigma t)] + b_{ij}(\sigma)[-\sigma \sin(\sigma t)], \tag{51}$$

with

$$m_{ij}(\sigma) = \text{added mass for modes } (ij) = \frac{\rho}{\sigma} \sum_{n=1}^{\infty} b_{nj} I_{ni}^{(2)},$$
$$b_{ij}(\sigma) = \text{damping coefficient for modes } (ij) = -\rho b_{0j} I_{0i}^{(2)}, \tag{52}$$

where $I_{ni}^{(2)}$ and $I_{0i}^{(2)}$ are defined for mode i according to equations (48b).

With the added mass and damping coefficients known from equations (52), the genuine added mass M_{ij} and retardation function K_{ij} can be obtained from equations (45). The choice of σ_1 is arbitrary, but a high-frequency σ_1 is preferable, since thereby the errors of discretization and integration are less important. Also, different values of σ_1 should be used to check that the M_{ij} value is constant.

For a single-degree-of-freedom system (as in Section 3.1) defined by, say, mode i, the procedure is identical to the above and the notation used is

$$F_h = F_{ii} = \text{hydrodynamic force},$$
$$M_h = M_{ii} = \text{'genuine' added mass},$$
$$K(\tau) = K_{ii}(\tau) = \text{retardation function}. \tag{53}$$

APPENDIX II: ASYMPTOTIC AND LIMITING CASE ANALYSIS FOR WAVEMAKER

For a single degree of freedom the equation for optimal motion of a wave absorber is given by equation (17):

$$M_h\ddot{a}(t) + \int_{-\infty}^{t} K(t-\tau)\dot{a}(\tau)\mathrm{d}\tau = F_1(t),$$

where M_h is the genuine or infinite frequency added mass and $K(\tau)$ is the retardation function given by equation (45a):

$$K(\tau) = \frac{2}{\pi}\int_0^\infty b(\sigma)\cos(\sigma\tau)\mathrm{d}\sigma.$$

The damping coefficient $b(\sigma)$ is determined as shown in Appendix I. Since the range of integration in equation (45a) is from zero to infinity, it is convenient to determine the retardation function as

$$K(\tau) = \frac{2}{\pi}\int_0^{\sigma_H} b(\sigma)\cos(\sigma\tau)\mathrm{d}\sigma + \frac{2}{\pi}\int_{\sigma_H}^\infty b_H(\sigma)\cos(\sigma\tau)\mathrm{d}\sigma, \tag{54}$$

where $b(\sigma)$ is determined as per Appendix I and $b_H(\sigma)$ is an approximation for $b(\sigma)$ for frequencies higher than a suitably high frequency σ_H. Our intent now is to determine the expression $b_H(\sigma)$ for the hinged and piston wavemakers.

The added mass and damping coefficient for a wavemaker operating sinusoidally at a frequency σ are given in Appendix I as

$$m_h(\sigma) = \frac{\rho}{\sigma}\sum_{n=1}^{\infty}\frac{\sigma}{k_n}\frac{I_n^{(2)}}{I_n^{(1)}}I_n^{(2)}, \tag{55}$$

$$b(\sigma) = -\rho b_0 I_0^{(2)} = \rho\frac{\sigma}{k_0}\frac{I_0^{(2)}}{I_0^{(1)}}I_0^{(2)}, \tag{56}$$

where

$$I_0^{(1)} = \int_{-h}^{0}\psi_0^2(y)\mathrm{d}y = \frac{h}{2}\left(1+\frac{\sinh(2k_0h)}{2k_0h}\right).$$

Case 1. Piston wavemaker

$$\delta(y) = 1 \qquad I_0^{(2)} = \frac{1}{k_0}\sinh(k_0h).$$

From equations (56)

$$b(\sigma) = \rho\frac{\sigma}{k_0}\frac{1}{k_0^2}\frac{\sinh^2(k_0h)}{I_0^{(1)}} = \frac{2\rho\sigma}{k_0^2}\frac{2\sinh^2(k_0h)}{2k_0h+\sinh(2k_0h)} = \frac{2\rho\sigma}{k_0^2}\frac{2\sinh^2(k_0h)}{2k_0h+2\sinh(k_0h)\cosh(k_0h)}.$$

Now, as $\sigma\to\infty$, $k_0h\ (=\sigma^2h/g)\to\infty$. Hence

$$b(\sigma)\to\frac{2\rho\sigma}{k_0^2} \quad \text{as } \sigma\to\infty.$$

For $\sigma\to\infty$, $\sigma^2=k_0h$ and therefore

$$b_H(\sigma)\approx\frac{2\rho g^2}{\sigma^3} \quad \text{as } \sigma\to\infty. \tag{57}$$

Case 2. Hinged wavemaker

$$\delta(y)=\frac{y+h}{h}, \qquad I_0^{(2)}=\frac{1}{hk_0^2}[k_0h\sinh(k_0h)+1-\cosh(k_0h)],$$

$$b(\sigma)=\rho\frac{\sigma}{k_0}\frac{I_0^{(2)}}{I_0^{(1)}}I_0^{(2)}=\rho\frac{\sigma}{k_0}\frac{1}{k_0^2}\frac{\sinh(k_0h)+[1-\cosh(k_0h)]/k_0h}{I_0^{(1)}}$$

$$=\frac{2\rho\sigma}{k_0^2}2\frac{\sinh^2(k_0h)+2\sinh(k_0h)[1-\cosh(k_0h)]/k_0h+[1-\cosh(k_0h)]/k_0h}{2k_0h+2\sinh(k_0h)\cos(k_0h)}.$$

As $\sigma\to\infty$, $kh\ (=\sigma^2h/g)\to\infty$ and hence

$$b_H(\sigma)\approx\frac{2\rho g^2}{\sigma^3} \quad \text{as } \sigma\to\infty. \tag{58}$$

Notes

1. There is no dependence of $b_H(\sigma)$ on h as $\sigma\to\infty$.
2. The asymptotic approximation is the same for both the hinged and the piston cases. This is because, the wavelength being so small, the wave cannot distinguish between the action of a piston and a hinged wavemaker. In general there is no dependence on the shape function of the wavemaker.

Very-low-frequency damping coefficient

A very-low-frequency approximation to the damping coefficient is derived here to be used for the verification of the results obtained from Appendix I. The damping coefficient is given by equation (56) as:

$$b(\sigma)=\rho\frac{\sigma}{k_0}\frac{I_0^{(2)}}{I_0^{(1)}}I_0^{(2)}.$$

As $\sigma\to0$, $\sigma^2=gk_0^2h$, i.e.

$$\sigma=k_0\sqrt{(gh)}.$$

and

$$I_0^{(1)}=\frac{h}{2}\left(1-\frac{\sinh(2k_0h)}{2k_0h}\right)\approx h. \tag{59}$$

Case 1. Hinged wavemaker

$$I_0^{(2)}=\frac{1}{k_0}\left(\sinh(k_0h)+\frac{1-\cosh(k_0h)}{k_0h}\right)\approx\frac{1}{k_0}\left(k_0h+\frac{(k_0h)^3}{3!}+\ldots+\frac{1-1-(k_0h)^2/2!+\ldots}{k_0h}\right)$$

$$\approx\frac{1}{k_0}\left(k_0h-\frac{k_0h}{2}\right)=\frac{h}{2}.$$

Hence, using equations (56) and (59), we get

$$b(\sigma)\approx\frac{\rho}{4}g^{4/2}h^{9/2} \quad \text{as } \sigma\to 0. \tag{60}$$

Case 2. Piston wavemaker

$$I_0^{(2)}=\frac{1}{k_0}\sinh(k_0h)\approx h \quad \text{as } \sigma\to 0.$$

Hence using equations (56) and (59), we get

$$b(\sigma)\approx\rho g^{1/2}h^{9/2}. \tag{61}$$

Infinite frequency added mass

The equation of the optimal motion of the wave absorber involves the determination of the infinite frequency added mass. This is determined as shown in equation (45) as

$$M_h=m_h(\sigma_1)-\frac{1}{\sigma_1}\int_0^\infty K(\tau)\sin(\sigma_1\tau)\mathrm{d}\tau,$$

where σ_1 is any frequency.

Alternatively, M_h can be determined by posing the boundary value problem (BVP) for $\sigma=\infty$. This would then serve as a check on the accuracy of $K(\tau)$.

BVP for infinite frequency. The free surface condition is[10]

$$\phi_{tt}+g\phi_y=0 \quad \text{on } y=0, \qquad \text{i.e. } -\omega^2\phi+g\phi_y=0.$$

This implies

$$\phi=0 \quad \text{as } \omega\to\infty. \tag{62}$$

Hence the BVP is that shown in Figure 13.

Now

$$\nabla^2\Phi=0. \tag{63}$$

Let $\Phi=\mathrm{Re}(\phi e^{-\mathrm{i}\omega t})$ and $\phi=X(x)\,Y(y)$ using separation of variables. Hence from equation (63) we get

$$\frac{X''}{X}+\frac{Y''}{Y}=0. \tag{64}$$

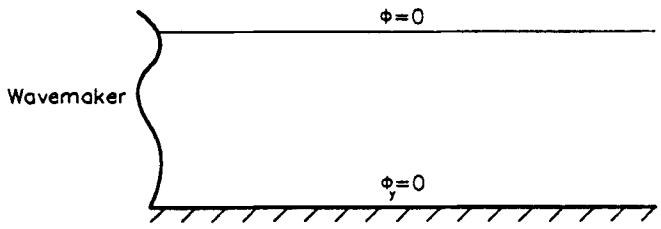

Figure 13. Definition sketch for infinite frequency BVP

Let $Y''/Y=B$. If $B=k^2>0$, then

$$Y=c\cosh(ky)+d\sinh(ky). \tag{65}$$

Clearly, to satisfy $\phi=0$ on $y=0$ and $\phi_y=0$ on $y=-h$ implies $c=d=0$.

If $B=-k^2<0$, then

$$Y=c\cos[k(y+h)]+d\sin[k(y+h)].$$

This finally yields the solution as

$$Y=\sum_{n=1}^{\infty} d_n\cos[k_n(y+h)], \tag{66}$$

where $k_nh=(2n-1)\pi/2$. Hence the solution for ϕ, imposing the condition of boundedness as $x\to\infty$, is

$$\phi=\sum_{n=1}^{\infty} A_n e^{-k_nx}\cos[k_n(y+h)].$$

The determination of the added mass proceeds as before and it can finally be put in the form

$$M_h=\rho\sum_{n=1}^{\infty}\frac{1}{k_n}\frac{I_n^{(2)}}{I_n^{(1)}}I_n^{(2)}, \tag{67}$$

where

$$I_n^{(1)}=\int_{-h}^{0}\psi_n^2(y)\mathrm{d}y, \qquad I_n^{(2)}=\int_{-h}^{0}\delta(y)\psi_n(y)\mathrm{d}y, \qquad \psi_n(y)=\cos[k_n(y+h)]. \tag{68}$$

APPENDIX III: NOTATION

$\dot{a}_i(t)$	absorber velocity in ith degree of freedom (refers to one-degree-of-freedom (d.o.f.) system if i is not denoted)
b_{0j}, b_{nj}	coefficients in expansion for velocity potential
C_ϕ	part of contour where ϕ is known
C_ψ	part of contour where ψ is known
C_{ϕ_t}	part of contour where ϕ_t is known
C_{ψ_t}	part of contour where ψ_t is known
E	energy flux
E_{L}	energy input to domain from left-side boundary
E_Ω	energy within domain Ω
E_{R}	energy leaving right-side boundary
F_{I}	wave-excitation force on absorber from inner domain
F_{O}	hydrodynamic force on absorber due to radiation potential
F_{ij}	force on absorber in d.o.f. i due to motion in d.o.f. j (also denoted as F_{O} for one-d.o.f. system)
$F_{i\mathrm{O}}$	wave-excitation force on absorber from inner domain for d.o.f. i
g	acceleration due to gravity
h	water depth
h_n	Volterra kernels
H_n	frequency domain response functions
$I_{ni}^{(1)}$, $I_{ni}^{(2)}$	integrals for nth eigenvalues and d.o.f. i
K_{ij}	retardation function in d.o.f. i for motion in d.o.f. j

k	wave number
M_h	'genuine' added mass for one-d.o.f. case
M_{ij}	'genuine' added mass in d.o.f. i for unit motion in d.o.f. j
p	pressure
p_s	pressure at the free surface
u, v	velocity components in x- and y-directions
w	complex velocity defined as $w=u-iv$
$x(y, t)$	absorber velocity in x-direction
$Y(\ )$	functional of a function
z	point in complex plane defined as $z=x+iy$

Greek letters

β	complex potential defined as $\beta=\phi+i\psi$
γ	retardation potential for unit velocity in d.o.f. i
$\delta_i(y)$	shape function of absorber in d.o.f. i
ρ	density of fluid
σ	wave frequency
Σ	boundary on domain Ω
Σ_L	left-side boundary
Σ_F	free surface boundary
Σ_R	right-side boundary
Σ_B	bottom boundary
ϕ	velocity potential
ϕ_I	incident velocity potential
ϕ_O	outer domain potential
$\phi_R^{(i)}$	radiation potential for d.o.f. i
ψ_O, ψ_h	vertical eigenfunctions
Ω	domain of definition

REFERENCES

1. R. W. Yeung, 'Numerical methods in free-surface flows', *Am. Rev. Fluid Mech.*, **14**, 395–442 (1982).
2. M. S. Longuet-Higgins and E. D. Cokelet, 'The deformation of steep surface waves on water, I. A numerical method of computation', *Proc. R. Soc. Lond. A*, **350**, 1–26 (1976).
3. T. Vinje and P. Brevig, 'Breaking waves on finite water depths, a numerical study', *Ships in rough Seas (SIS) Report*, Division of Marine Hydrodynamics, Norwegian Institute of Technology, 1980.
4. S. Jagannathan, 'Non-linear free surface flows and an application of the Orlanski boundary condition', *Int. j. numer. methods fluids*, **8**, 1051–1070 (1988).
5. G. W. Hedstrom, 'Nonreflecting boundary conditions for nonlinear hyperbolic systems', *J. Comput. Phys.*, **30**, 222–237 (1979).
6. D. H. Rudy and J. C. Strikwerda, 'A nonreflecting outflow boundary for subsonic Navier–Stokes calculations', *J. Comput. Phys.*, **36**, 55–70 (1980).
7. B. Engquist and A. Majda, 'Absorbing boundary conditions for the numerical simulation of waves', *Math. Comput.*, **31**, 629–651 (1977).
8. S. Jagannathan, 'Nonlinear free surface flows and open boundary conditions', *Ph.D. Dissertation*, University of California, Berkeley, 1985.
9. F. John, 'On the motion of floating bodies—I', *Commun. Pure Appl. Math.*, **2**, 13–57 (1949).
10. J. V. Wehausen and E. V. Laitone, 'Surface waves', in S. Flugge (ed.), *Handbuch der Physik, Vol IX*, Springer, Berlin, 1960, pp. 446–778.
11. W. E. Cummins, 'The impulse response function and ship motions', *Schiffstechnik*, **9**, 101–109 (1962).
12. R. E. D. Bishop, R. K. Burcher and W. G. Price, 'The uses of functional analysis in ship dynamics', *Proc. R. Soc. Lond. A*, (1973).
13. R. E. D. Bishop, R. K. Burcher and W. G. Price, 'Application of functional analysis to oscillatory ship model testing', *Proc. R. Soc. Lond. A*, (1973).
14. C. L. S. Guo, 'Non-linear theory of ship maneuvering', *Ph.D. Dissertation*, University of California, Berkeley, 1985.